Journal of the European Ceramic Society **17** (1997) 575–580

PII: S0955-2219(96)00093-3
0955-2219/97/$17.00

On the Extension of the α-SiAlON Solid Solution Range and Anisotropic Grain Growth in Sm-Doped α-SiAlON Ceramics

Lars-Olov Nordberg,[a] Zhijian Shen,[b] Mats Nygren[a,*] & Thommy Ekström[a]

[a]Department of Inorganic Chemistry, Arrhenius Laboratory, University of Stockholm, S-10691 Stockholm, Sweden
[b]Department of Material Science and Engineering, Zhejiang University, Hangzhou 310027, People's Republic of China

(Received 6 March 1996; revised version received 15 April 1996; accepted 3 May 1996)

Abstract

α-SiAlON samples of the overall composition $Sm_xSi_{12-(m+n)}Al_{m+n}O_nN_{16-n}$ *with* m *and* n *in the ranges* $0{\cdot}6 \leq m \leq 1{\cdot}44$ *and* $1{\cdot}3 \leq n \leq 1{\cdot}7$ ($m = 3x$), *were prepared by a hot-pressing technique at 1800 and 1700°C. Based on X-ray powder diffraction studies and elemental analysis of individual α-SiAlON grains in the obtained ceramic compacts, the extension of the Sm-doped α-SiAlON solid solution range was mapped out. The* m*-value was found to vary between 0·89 and 1·52 while* n *was always less than 1·23. Elongated α-SiAlON grains were found preferentially in compacts having overall compositions located slightly outside the oxygen-rich border-line of the homogeneity region of the Sm-doped α-SiAlON phase, i.e. for* $m \approx 1{\cdot}2$ *and* $n \approx 1{\cdot}3$. *We also noticed that elongated α-SiAlON grains were formed preferentially perpendicular to the pressure applied in the sintering procedure. All samples exhibited HV10-values in the range 21–22 GPa and* K_{Ic}*-values in the range 4·0–4·7 MPa* $m^{1/2}$. © *1997. Published by Elsevier Science Limited. All rights reserved.*

1 Introduction

The general formula of the α-SiAlON phase can be expressed as $R_xSi_{12-(m+n)}Al_{m+n}O_nN_{16-n}$, where m(Si–N) are replaced by m(Al–N) and n(Si–N) by n(Al–O) units.[1] The introduced valence discrepancy is compensated by $x = m/3$ rare-earth R^{3+} elements. Thus, the α-SiAlON solid solution range has a two-dimensional extension in the plane Si_3N_4–Al_2O_3·AlN–RN·3AlN located in the commonly used Jänecke prism that illustrates the phase relations of the particular R–Si–Al–O–N system. A detailed picture of the extension of the α-SiAlON phase area is only known for R = Y.[2] Studies of the subsolidus phase relationships in Si_3N_4–AlN–rare-earth oxide systems have suggested that all rare-earth stabilized α-SiAlONs have quite similar composition areas.[3,4] Recent studies concerning the thermal stability of Sm-doped α-SiAlON ceramics have, however, indicated that in the Sm-doped SiAlON system the α-SiAlON compositional area is smaller than in the Y–SiAlON system.[5] These findings initiated further studies of the Sm–α-SiAlON system and in this article the α-SiAlON compositional area is mapped out as it is revealed by phase analysis based on X-ray diffraction data and elemental analysis of individual α-SiAlON grains in samples with overall compositions close to the known Y-doped α-SiAlON compositional area and prepared at 1800 and 1700°C by the hot-pressing technique.

It is well known that α–β SiAlON ceramics normally contain equiaxed α-SiAlON grains, β-SiAlON grains with an elongated shape and amorphous or crystalline intergranular phase(s). In α–β SiAlON ceramics the α-SiAlON grains contribute to the hardness while the presence of elongated β-SiAlON grains is believed to improve the fracture toughness.[6] There are very few reports on the formation of elongated α-SiAlON grains, but recent studies of the thermal stability of different rare-earth doped α-SiAlON phases have revealed that elongated α-SiAlON grains can be formed under certain preparative conditions.[5,7–10] Hwang *et al.* have also observed anisotropic grain growth of the α-SiAlON phase when different sintering aids (CaO, SrO and Y_2O_3) are used simultaneously.[11] In this contribution we describe the preparation conditions used to produce elongated Sm-doped α-SiAlON grains and evaluate their impact on the mechanical properties, i.e. find out whether the presence of elongated α-SiAlON grains will improve the fracture toughness of the material.

*To whom correspondence should be addressed.

Table 1. Designed overall compositions, sintering conditions applied and densities of the hot-pressed samples

Sample no.	*Designed composition*			*Overall weight percent*				*Actual formula*	*Sintering condition (temp/time)*	*Density (g cm^{-3})*
	m	n	x	Si_3N_4	AlN	Al_2O_3	Sm_2O_3			
1	0·6	1·3	0·2	80·3	10·8	3·0	5·9	$Sm_{0.2}Si_{10.90}Al_{1.90}O_{1.29}N_{14.69}$	1800°C/2 h	3·34
2	1·05	1·7	0·35	70·9	15·2	4·0	9·9	$Sm_{0.35}Si_{9.29}Al_{2.76}O_{1.70}N_{14.36}$	1800°C/2 h	3·37
3	1·05	1·3	0·35	74·0	14·4	1·7	9·9	$Sm_{0.35}Si_{9.70}Al_{2.36}O_{1.30}N_{14.78}$	1800°C/2 h	3·37
4	1·44	1·3	0·48	67·1	19·3	0·7	12·9	$Sm_{0.48}Si_{9.25}Al_{3.13}O_{1.32}N_{15.07}$	1800°C/2 h	3·40
3a	1·05	1·3	0·35	74·0	14·4	1·7	9·9	$Sm_{0.35}Si_{9.70}Al_{2.36}O_{1.30}N_{14.78}$	1700°C/1 h	3·35
3b	1·05	1·3	0·35	74·0	14·4	1·7	9·9	$Sm_{0.35}Si_{9.70}Al_{2.36}O_{1.30}N_{14.78}$	1700°C/2 h	3·37
3c	1·05	1·3	0·35	74·0	14·4	1·7	9·9	$Sm_{0.35}Si_{9.70}Al_{2.36}O_{1.30}N_{14.78}$	1700°C/4 h	3·40

2 Experimental

The overall compositions of the samples prepared in the present study are given in Table 1. Their positions in the Si_3N_4-rich corner of the plane Si_3N_4–SmN·3AlN–(4/3)(AlN·Al_2O_3) are given in Fig. 1(a). The samples with the overall compositions $Sm_xSi_{12-4.5x}Al_{4.5x}O_{1.5x}N_{16-1.5x}$ with x = 0·25, 0·35, 0·40, 0·60, 0·70, 0·80 and 1·0, prepared as described in Ref. 5, are also represented in the same figure. The extension of the Y-doped α-SiAlON

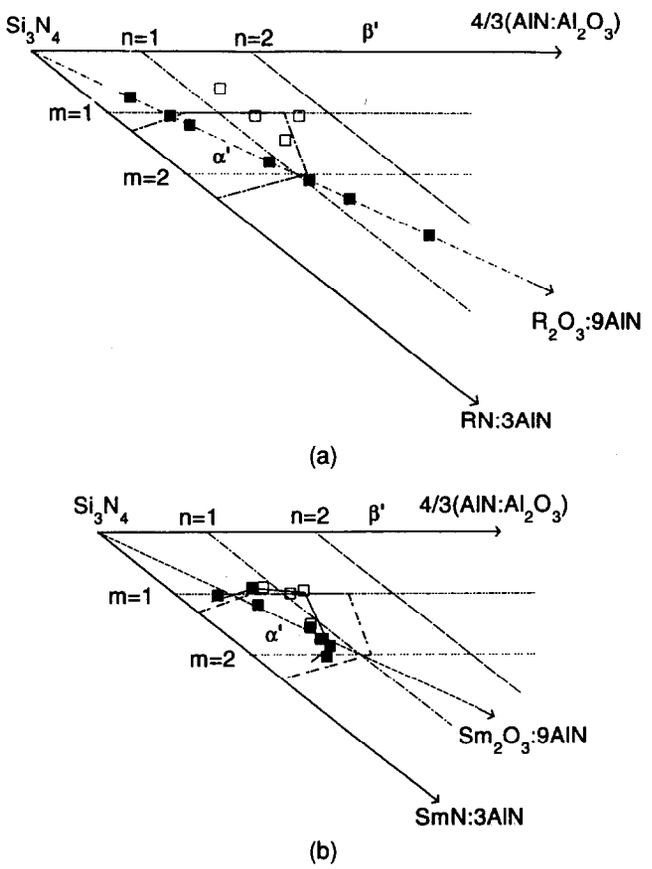

Fig. 1. (a) The Si_3N_4-rich corner of the subsolidus phase relationship in the R–Si–Al–O–N system, showing the overall compositions of the prepared samples (□) and the overall compositions of the samples $Sm_xSi_{12-4.5x}Al_{4.5x}O_{1.5x}N_{16-1.5x}$ prepared as described in Ref. 5 (■); the α-SiAlON forming region for Y as given by Sun *et al.*[2] is also marked as dashed line. (b) The EDS measured composition of individual α-SiAlON grains in the samples given in Fig. 1(a).

phase area, as determined by Sun *et al.*,[2] is given by the dotted line in Fig. 1(a). The starting materials were Si_3N_4 (UBE SN10E), Al_2O_3 (Alcoa SG30), AlN (HC Starck-Berlin, grade A) and Sm_2O_3 (HC Starck-Berlin, grade finest). When calculating the compositions of the samples, corrections were made for the small amounts of oxygen present in the Si_3N_4 and AlN raw materials.

The starting materials, in batches of 30 g, were ball-milled in water-free propanol for 24 h using sialon milling media. Compacted pellets of dried powders were hot-pressed (HP) in nitrogen at 1800°C for 2 h and at 1700°C for 1–4 h, at a pressure of 30 MPa in a graphite resistance furnace. After the sintering procedure the samples were allowed to cool inside the furnace at a rate of ~ 50°C min.$^{-1}$

The density was measured in water according to Archimedes' principle. Hardness (HV10) and indentation fracture toughness (K_{Ic}) at room temperature were obtained on carefully polished specimens with a Vickers diamond indenter applying a 98 N load. The fracture toughness was evaluated with the formula given by Anstis *et al.*,[12] with a value of 300 GPa for Young's modulus.

Crystalline phases were characterized by their X-ray powder diffraction (XRD) patterns obtained in a Guinier–Hägg camera with Si as internal standard, using monochromatic Cu K_{α_1} radiation. X-ray films were evaluated by means of the SCANPI system,[13] and the unit cell parameters were determined with the PIRUM computer software.[14] The obtained unit cell parameters of the β-SiAlON phase, $Si_{6-z}Al_zO_zN_{8-z}$, were used to calculate its z-value using the equations given in Ref. 15. In the estimation of the amounts of crystalline phases, the integrated intensities of the following peaks were used: (102) and (210) of the α-SiAlON, (101) and (210) of the β-SiAlON, and (101) and (012) of 21R. The relative weight fraction of each phase was then calculated from the expression:

$$W_k = (I_k/K_k) \sum_{i=1}^{n} (I_i/K_i) \qquad 1 \le k \le n \qquad (1)$$

where W_k is the weight fraction of phase k, n is the number of crystalline phases present, I_i is the intensity of the selected reflection (hkl) of phase i and K_i are constants determined from experimental calibration curves. The X-ray diffraction patterns of sintered compacts were obtained with a STOE diffractometer (Stadi-P). Diffraction patterns were recorded for sample 3 oriented perpendicular and parallel to the hot-pressing direction.

Polished surfaces of the prepared samples were examined in scanning electron microscopes (Jeol JSM 820 and 880) equipped with energy-dispersive spectrometers (Link AN 10000). The compositions of the various phases given below have been determined with use of calibration curves, and they represent mean values from at least five point measurements.

3 Results and Discussion

The samples hot-pressed (HPed) at 1800 and 1700°C were all found to be fully densified, as revealed by optical and scanning electron microscopy studies. The variation in density with sintering time, temperature and composition (see Table 1) can easily be understood in terms of the variable content of α- and β-SiAlON and crystalline and/or amorphous intergranular phase(s) in the samples.

3.1 Phase analysis and solid solubility limits of Sm-doped α-SiAlON

The phases present, the cell parameters of the α- and β-SiAlON phases and the z-value of the latter in the various samples are given in Table 2. According to Fig. 1(a), sample 1 is expected to contain α- and β-SiAlON in approximately equal proportions, in accordance with the findings. Sample 2 should mainly contain the α-SiAlON phase but does contain small amounts of the β-SiAlON and 21R phases as well. Finally, in samples 3 and 4, the only expected crystalline phase is α-SiAlON, but sample 4 does contain appreciable amounts of the 21R phase.

The compositions of individual α-SiAlON grains measured by energy-dispersive spectroscopy (EDS) in samples 1–4 are given in Table 2 and Fig. 1(b). Corresponding data for the samples with overall composition $Sm_xSi_{12-4.5x}Al_{4.5x}O_{1.5x}N_{16-1.5x}$ with x = 0·25, 0·35, 0·40, 0·60, 0·70, 0·80 and 1·0 (obtained from Ref. 5) are reproduced in Fig. 1(b). It is quite evident from Fig. 1(b) and the phase analysis described above that the compositional area of the α-SiAlON phase is smaller in the Sm–SiAlON system than that in the corresponding Y–system. The m-values in the general formula of the α-SiAlON phase, $R_xSi_{12-(m+n)}Al_{m+n}O_nN_{16-n}$, are very similar in the two systems and thus also are the x-values, while the Sm-doped α-SiAlON phase seems not to be able to accommodate as much oxygen in its network as its yttrium analogue, i.e. $n_{Sm} < n_Y$. In our previous study of the Sm-doped α-SiAlON system it was concluded that melilite was easily formed as an intergranular crystalline phase during the cooling part of the sintering cycle especially in samples where x in $Sm_xSi_{12-4.5x}Al_{4.5x}O_{1.5x}N_{16-1.5x}$ is equal to or exceeds 0·6. In order to avoid the formation of melilite, rather fast cooling rates had to be applied.[5] The samples prepared in this study have all x-values less than 0·6 and comparatively low cooling rates have been used. The fact that no melilite phase is formed in samples 1–4 seems to indicate that the formation of melilite is retarded in the compositional region x <0·6.

3.2 Microstructure and morphology of α-sialon grains

Scanning electron micrographs of samples 1–4 prepared at 1800°C, recorded in back-scattered electron mode, are shown in Figs 2(a)–(e). The β-SiAlON and the 21R (Si;Al)(O;N)-polytype appear with dark black contrast (which in turn can be differentiated by Al/Si elemental analysis), the α-SiAlON phase appears with medium grey and the Sm-enriched intergranular phase with bright phase contrasts. Comparing the microstructures of the different samples the following can be noticed:

Table 2. Phase content, unit cell dimensions and EDS measured composition of the α-sialon phase in the prepared samples

Sample no.	*Crystalline phases*			*α-sialon unit cell*		*β-sialon unit cell*			*EDS α-sialon composition*		
	α	β	*21R*	a(Å)	c(Å)	a(Å)	c(Å)	z	m	n	x
1	55	45		7·8059(4)	5·6859(4)	7·6245(4)	2·9236(3)	0·7	0·89	0·89	0·30
2	90	5	5	7·8135(4)	5·6942(4)				0·95	1·23	0·32
3	100			7·8125(3)	5·6920(4)				0·99	1·07	0·33
4	92		8	7·8292(3)	5·7074(4)				1·52	0·88	0·51
3a	100			7·8133(4)	5·6927(4)						
3b	100			7·8130(3)	5·6934(4)						
3c	100			7·8105(4)	5·6925(4)						

(1) The micrograph of sample 1 [see Fig. 2(a)] shows that, in addition to a small amount of a residual intergranular phase, it contained approximately the same amount of α- and β-SiAlON in accordance with the X-ray analysis. The α-SiAlON grains are equiaxed while the β-SiAlON grains mostly exhibit elongated shape.
(2) The micrograph of sample 2 [see Fig. 2(b), recorded in conjunction with elemental analysis] reveals the presence of three different phases: (i) elongated β-SiAlON grains; (ii) stacked bundles of the 21R-polytype; (iii) α-sialon grains with three different morphologies, namely small equiaxed grains, large anisotropic ones and elongated grains with a larger aspect ratio. The micrograph also reveals that this sample contains a large amount of amorphous intergranular phase.

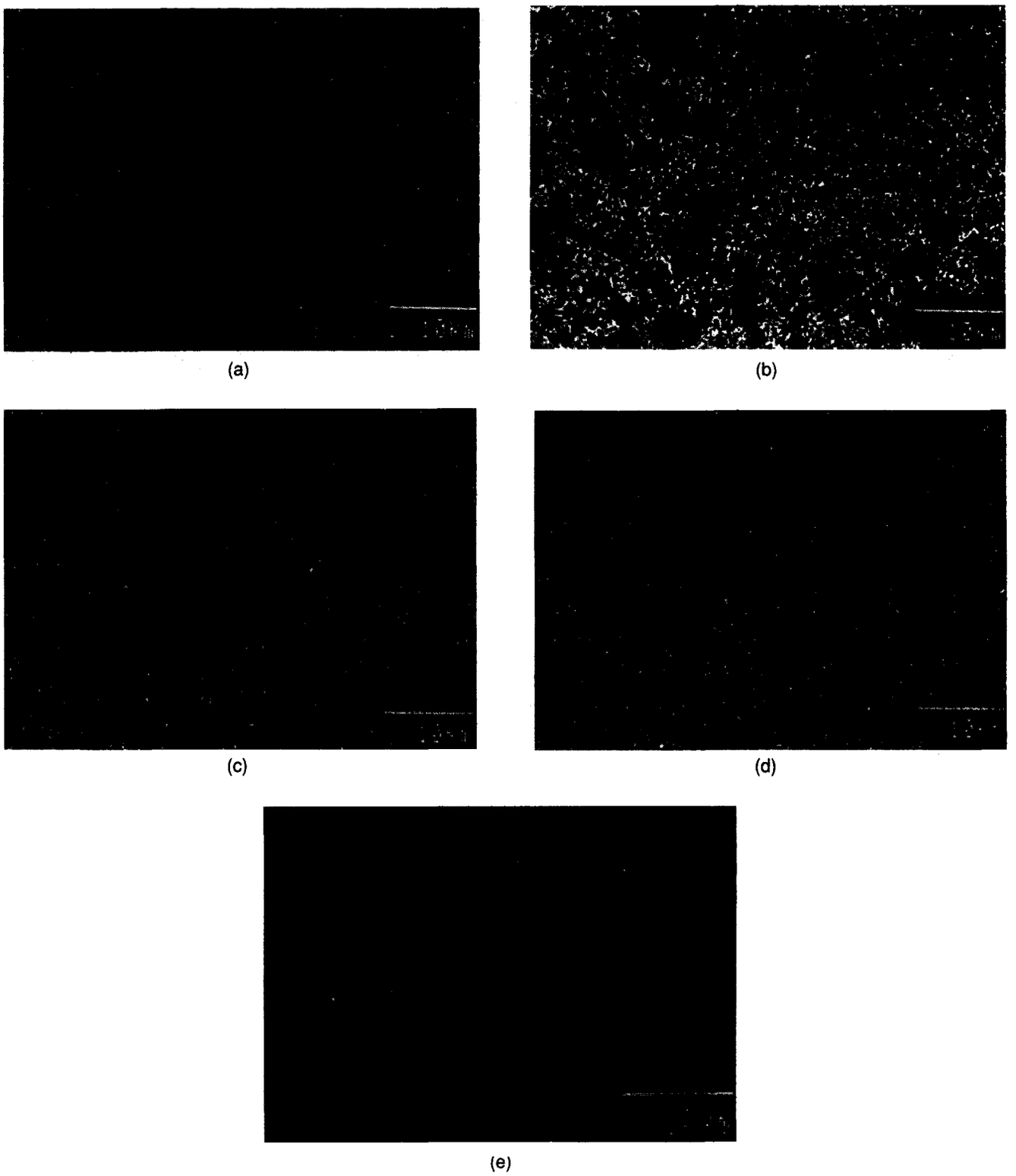

Fig. 2. Back-scattered SEM micrographs showing the microstructure of sample 1 (a), sample 2 (b), sample 3 (c) and sample 4 (d) on the surface oriented parallel to the sintering pressure direction, as well as sample 3 (e) on the surface oriented perpendicular to the sintering pressure direction.

(3) The micrograph of sample 3 [Fig. 2(c)], having an overall composition of $x = 0{\cdot}35$ and $n = 1{\cdot}3$, shows that this sample is almost a single-phase α-SiAlON ceramic but small amounts of a black phase are also found and confirmed to be the 21R-polytype by elemental analysis. The α-SiAlON grains in this sample have an elongated shape, but fine equiaxed α-SiAlON grains are also present. This micrograph is recorded for a sample having its polished surface parallel to the pressure applied in the sintering procedure. The micrograph given in Fig. 2(e) also emanates from sample 3, but in this case the surface exposed was perpendicular to the applied sintering pressure. The phases present are the same as those in Fig. 2(c), but slightly more elongated α-SiAlON grains are found.

(4) Sample 4 [see Fig. 2(d)], having an overall x-value of 0·48 and an n-value of 1·3, contains two phases: α-SiAlON and larger amount of the 21R-polytype than in the other studied samples. The α-SiAlON grains exhibit elongated as well as equiaxed shapes.

The microstructure of sample 3 prepared at 1700°C was very similar to the one obtained at 1800°C, i.e. elongated α-SiAlON grains were found in amounts increasing with increasing sintering time but in lesser amounts than in the sample prepared at 1800°C.

The XRD pattern of the crushed powder of sample 3, obtained in a Guinier–Hägg camera, is given in Fig. 3. Corresponding records from the compact of the same composition, obtained in the STOE diffractometer (working in reflection mode) with the exposed surface oriented perpendicular and parallel to the applied sintering pressure, are also given in Fig. 3. The intensities of the (1 0 2) and (2 1 0) reflections in the powder pattern are similar, as expected. The intensity of (2 1 0) is higher than that of (1 0 2) in the diffraction pattern obtained with the surface oriented perpendicular to the pressure direction, while the reverse is true for the surface oriented parallel to the pressure direction.

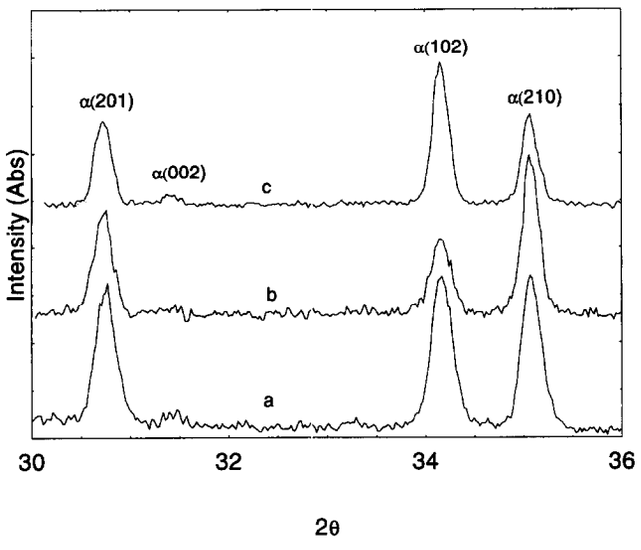

Fig. 3. X-ray powder pattern of sample 3 (a) and diffraction pattern obtained in reflection mode for the same solid ceramic compact on the surface oriented perpendicular (b) and parallel (c) to the applied pressure during the sintering process.

These observations suggest that the growth direction is along the c-axis of the unit cell of the α-SiAlON phase and that pressure promotes the growth of elongated α-SiAlON grains in a direction perpendicular to the applied pressure. The SEM–EDS studies showed that elongated α-SiAlON grains were preferentially formed in the samples with an overall composition of $n \approx 1{\cdot}3$ and $1 \leq m \leq 1{\cdot}44$. It can also be noted that all individual α-SiAlON grains had approximately the same n-value, i.e. $n \approx 1$. Anisotropic grain growth was also found in samples having an overall composition of $Sm_xSi_{12-4.5x}Al_{4.5x}O_{1.5x}N_{16-1.5x}$ with $x \geq 0{\cdot}6$.[5] These findings suggest that anistropic grain growth of the α-SiAlON phase is promoted by the presence of a liquid which is rich in oxygen and aluminium. This is in agreement with the findings by Cao *et al.* that nucleation of the α-SiAlON phase occurs more easily in an aluminium-rich liquid than in a aluminium-poor one.[16] It is not clear from this study whether the anisotropic grain growth is diffusion- or reaction-controlled, but there are reports stating that the grain growth of β-Si_3N_4 and β-SiAlON is diffusion-controlled.[17–20]

3.3 Mechanical properties

The hardness and fracture toughness of samples 1–4 are given in Table 3. Firstly it can be concluded that all samples exhibited HV10-values in the range 21–22 GPa and fracture toughness values in the range 4·0–4·7 MPa $m^{1/2}$ implying that no systematic variation with overall composition, sintering time and temperature can be discerned. Similar HV10- and K_{Ic}-values have been found for the samples of the overall composition

Table 3. Hardness and fracture toughness

Sample no.	*HV10 (GPa)*	K_{Ic} *(MPa* $m^{1/2}$*)*
1 ∥	21	4·4
1 ⊥	21	4·7
2 ∥	21	4·0
2 ⊥	21	4·3
3 ∥	22	4·0
3 ⊥	22	4·1
4 ∥	21	4·2
4 ⊥	21	4·2

⊥ and ∥ refer to data obtained with the surface oriented perpendicular and parallel to the pressure direction, respectively.

Fig. 4. A crack propagating in sample 3, which is deflected when it approaches the α-SiAlON grains at a low angle while it penetrates the grain when it propagates perpendicular to an elongated α-SiAlON grain.

$Sm_xSi_{12-4\cdot5x}Al_{4\cdot5x}O_{1\cdot5x}N_{16-1\cdot5x}$ with $0{\cdot}25 \leq x \leq 1{\cdot}0$.[5] It can also be noticed that when propagating cracks approach the α-SiAlON grains at a low angle they are deflected, but when they propagate perpendicular to an elongated α-SiAlON grain they are not deflected but penetrate the grain, as seen in Fig. 4. This behaviour suggests that the bonding at the interface between the α-SiAlON grains and the intergranular glassy phase is too strong to allow crack deflection in the latter case.

4 Conclusions

The solid solubility area of the Sm-doped α-SiAlON phase is somewhat smaller than its yttrium analogue. Anisotropic α-SiAlON grains are formed preferentially in samples with an overall composition close to the solubility area of the α-SiAlON phase in the oxygen-, aluminium- and yttrium-rich parts, respectively, i.e. for $n \approx 1$ and $1 \leq m \leq 1{\cdot}44$ and $x \geq 0{\cdot}6$ in $Sm_xSi_{12-4\cdot5x}Al_{4\cdot5x}O_{1\cdot5x}N_{16-1\cdot5x}$. No systematic variation of mechanical properties with the overall composition, size and shape of the α-SiAlON grains, sintering time and temperature could be discerned.

Acknowledgement

Financial support by the Swedish Research Council for Engineering Science is gratefully acknowledged.

References

1. Cao, G. Z. & Metselaar, R., α-SiAlON ceramics: a review. *Chem. Mater.*, **3** (1991) 242–252.
2. Sun, W. Y., Tien, T. Y. & Yen, T.-S., Solubility limits of α'-sialon solid solutions in the system Si, Al, Y/N, O. *J. Am. Ceram. Soc.*, **74** (1991) 2547–2550.
3. Sun, W. Y., Yen, D. S., Gao, L., Mandal, H., Liddell, K. & Thompson, D. P., Subsolidus phase relationships in Ln_2O_3–Si_3N_4–AlN–Al_2O_3 (Ln=Nd, Sm). *J. Eur. Ceram. Soc.*, **15** (1995) 349–355.
4. Huang, Z. K., Tien, T. Y. & Yen, T. S., Subsolidus phase relationships in Si_3N_4–AlN–rare earth oxide systems. *J. Am. Ceram. Soc.*, **69** (1986) C-241–C-242.
5. Shen, Z., Ekström, T. & Nygren, M., Temperature stability of samarium-doped α-sialon ceramics. *J. Eur. Ceram. Soc.*, **16** (1996) 43–53.
6. Ekström, T. & Nygren, M., SiAlON ceramics. *J. Am. Ceram. Soc.*, **75** (1992) 259–276.
7. Shen, Z., Ekström, T. & Nygren, M., Ytterbium stabilised α-sialon ceramics. *J. Phys. D: Appl. Phys.*, **296** (1996) 893–904.
8. Shen, Z., Ekström, T. & Nygren, M., Homogeneity region and thermal stability of neodymium doped α-sialon ceramics. *J. Am. Ceram. Soc.*, **79** (1996) 721–732.
9. Shen, Z., Ekström, T. & Nygren, M., Preparation and properties of stable dysprosium doped α-sialon ceramics. *J. Mater. Sci.*, in press.
10. Nordberg, L.-O. & Esktröm, T., Hot-pressed $MoSi_2$-particulate-reinforced α-SiAlON composites. *J. Am. Ceram. Soc.*, **78**[3] (1995) 797–800.
11. Hwang, C. J., Susintzky, D. W. & Beaman, D. R., Preparation of multication α-SiAlON containing strontium. *J. Am. Ceram. Soc.*, **78**[3] (1995) 588–592.
12. Anstis, G. R., Chantikul, P., Lawn, B. R. & Marshall, D. P., A critical evaluation of indentation techniques for measuring fracture toughness: I, Direct crack measurements. *J. Am. Ceram. Soc.*, **64** (1981) 533–538.
13. Johansson, K.-E., Palm, T. & Werner, P.-E., An automatic microdensitometer for X-ray powder diffraction photographs. *J. Phys.*,, **E13** (1980) 1289–1291.
14. Werner, P.-E., A Fortran program for least-squares refinement of crystal structure cell dimension. *Arkiv für Kemi*, **31**(43) (1969) 513.
15. Ekström, T., Käll, P.-O., Nygren, M. & Olsson, P.-O. Single-phase β-sialon ceramics by glass-encapsulated hot isostatic pressing. *J. Mater. Sci.*, **24** (1989) 1853–1861.
16. Cao, G. Z., Metselaar, R. & Ziegler, G., Formation and densification of α'-SiAlON ceramics. In *Ceramics Today — Tomorrows Ceramics*, ed. P. Vincenzini. Elsevier, 1991, pp. 1285–1293.
17. Hoffmann, M. J., Analysis of microstructural development and mechanical properties of Si_3N_4 ceramics. In *Tailoring of Mechanical Properties of Si_3N_4 Ceramics*, eds M. J. Hoffmann & G. Petzov. Kluwer, 1994, pp. 59–72.
18. Einarsrud, M.-A. & Mitomo, M., Mechanism of grain growth of β-SiAlON. *J. Am. Ceram. Soc.*, **76**[6] (1993) 1624–1626.
19. Hwang, S.-L. & Chen, I.-W., Nucleation and growth of β'-SiAlON. *J. Am. Ceram. Soc.*, **77**[7] (1994) 1719–1278.
20. Hwang, C. J. & Tien, T.-Y., Microstructural development in silicon nitride ceramics. *Mater. Sci. Forum*, **47** (1989) 84–109.